Cell

Opposing Dopaminergic and GABAergic Neurons Control the Duration and Persistence of Copulation in *Drosophila*

Michael A. Crickmore[1,3] and Leslie B. Vosshall[1,2,*]
[1]Laboratory of Neurogenetics and Behavior
[2]Howard Hughes Medical Institute
The Rockefeller University, 1230 York Avenue, Box 63, New York, NY 10065, USA
[3]Present address: Department of Neurobiology, Harvard Medical School, 220 Longwood Avenue, Boston, MA 02115, USA
*Correspondence: leslie.vosshall@rockefeller.edu
http://dx.doi.org/10.1016/j.cell.2013.09.055

SUMMARY

Behavioral persistence is a major factor in determining when and under which circumstances animals will terminate their current activity and transition into more profitable, appropriate, or urgent behavior. We show that, for the first 5 min of copulation in *Drosophila*, stressful stimuli do not interrupt mating, whereas 10 min later, even minor perturbations are sufficient to terminate copulation. This decline in persistence occurs as the probability of successful mating increases and is promoted by approximately eight sexually dimorphic, GABAergic interneurons of the male abdominal ganglion. When these interneurons were silenced, persistence increased and males copulated far longer than required for successful mating. When these interneurons were stimulated, persistence decreased and copulations were shortened. In contrast, dopaminergic neurons of the ventral nerve cord promote copulation persistence and extend copulation duration. Thus, copulation duration in *Drosophila* is a product of gradually declining persistence controlled by opposing neuronal populations using conserved neurotransmission systems.

INTRODUCTION

The selection of appropriate behavior can be central to organismal success, in part because the performance of one behavior often excludes other potentially profitable activities. It follows that not only the selection but also the duration of individual behaviors is critical. The durations of behaviors are determined by interactions between the internal state of the animal and information from the external environment. The external world is constantly changing, and internal states are equally dynamic (Atkinson and Birch, 1970). Time spent abstaining from a behavior often increases its associated drive, and the propensity to persist in a behavior often decreases with time spent performing the behavior. The neuronal processes underlying changes in persistence over time and integration of internal state with the external world are poorly understood.

The durations of most animal behaviors lie on the interval time scale: from hundreds of milliseconds to a few hours (Buhusi and Meck, 2005). The ability of animals to sense time on the interval scale was perhaps first documented in dogs by Pavlov (1927) and has recently been demonstrated in bees (Boisvert and Sherry, 2006), suggesting the existence of interval timing mechanisms throughout the animal kingdom. One behavior that takes place over a wide range of interval time is copulation, which ranges from ~1.5 s in rabbits (Rubin and Azrin, 1967) to 2–3 hr in the praying mantis (Prokop and Vaclav, 2005). Even within a genus, copulation lengths can vary dramatically from 40 s in *Drosophila robusta* (Grant, 1983) to 40 min in *Drosophila immigrans* (Grant, 1983). However, within a given species, copulation times can be highly reproducible, implying robust timing mechanisms.

To investigate neuronal timekeeping on the interval scale, we studied the neural basis of copulation duration in *Drosophila melanogaster* (27.7 ± 0.7 min with an SD of 4.4 min in our wild-type Berlin stock). We provide evidence that a primary determinant of copulation duration is the persistence of the male to continue mating. This persistence declines over the course of a mating and interacts with information from the external environment to determine when copulation will cease. Because persistence decreases as the probability of successful mating increases, it serves as a critical component in an apparent cost-benefit analysis weighing the advantages of continued mating versus engaging in alternative behaviors. We show that the decrease in persistence is promoted by ~8 GABAergic interneurons of the abdominal ganglion and opposed by dopaminergic neurons of the ventral nerve cord. The simplicity of this behavior, together with the small populations of neurons with conserved neurotransmission systems identified here, makes copulation duration an attractive model for studying neural coding of time and persistence.

RESULTS

A Gal4 Line that Labels Copulation Duration Neurons

We carried out a screen for male flies that spend a disproportionate amount of time in copulation (see Experimental

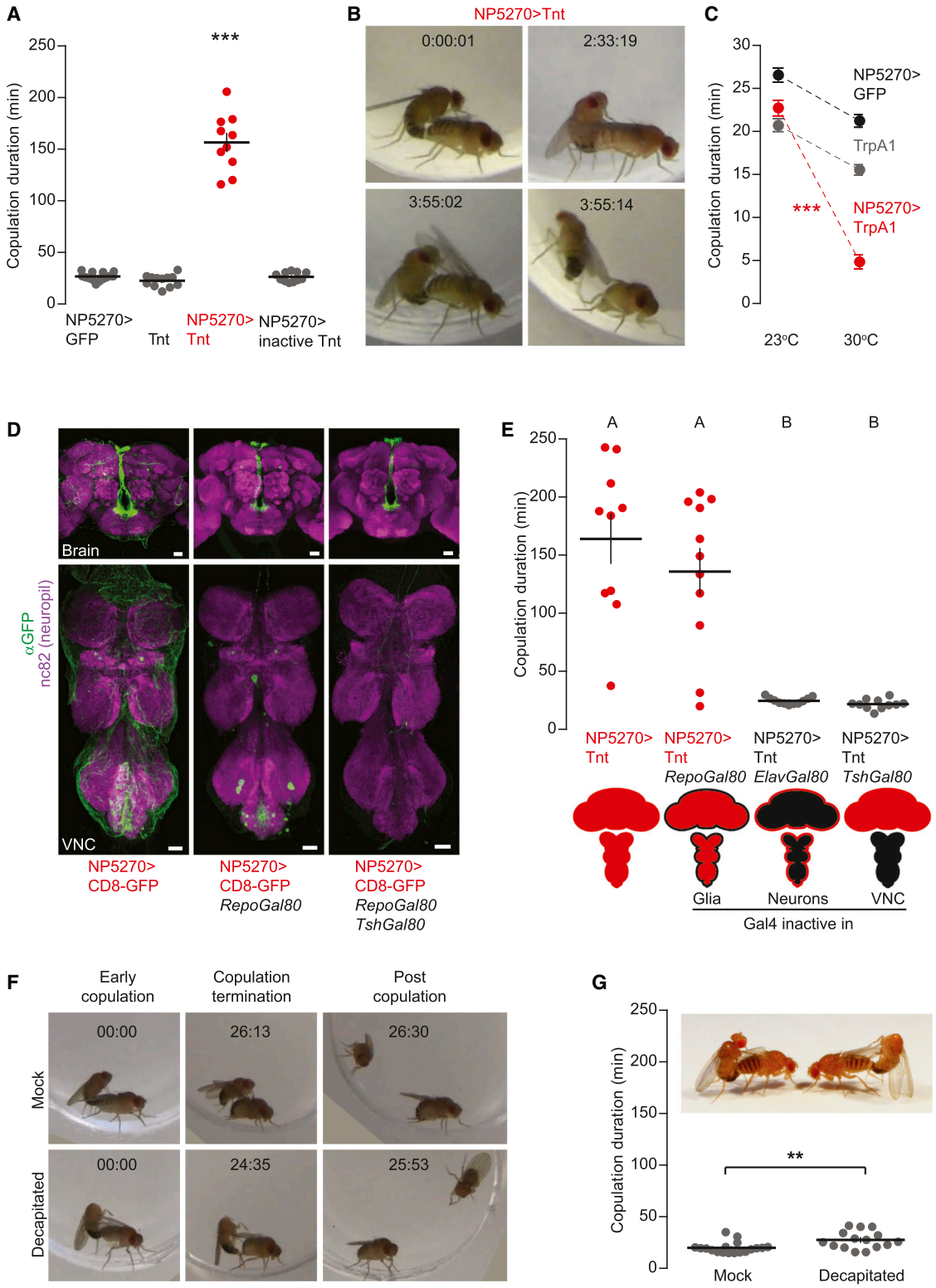

Figure 1. NP5270-Gal4 Labels Neurons that Control Copulation Duration

(A) Copulation durations of matings between w^{1118} females and males of the indicated genotype (***p < 0.001, one-way ANOVA with Tukey posttest; mean ± SEM, n = 10–16). Detailed information about fly genotypes in this and other figures is in the Extended Experimental Procedures.

(B) Video stills from a copulation with a NP5270 > Tnt male.

(legend continued on next page)

Procedures) by using the Gal4/UAS system (Brand and Perrimon, 1993) to inactivate neurons by selective expression of the tetanus toxin light chain (Tnt). Tnt blocks most evoked synaptic neurotransmission by cleaving neuronal synaptobrevin (Sweeney et al., 1995). We found a Gal4 line (NP5270 > Tnt) that caused males to spend, on average, six times longer in each copulation (Figure 1A). Copulation lengthening was not seen with mutant inactive Tnt, which lacks proteolytic activity (Sweeney et al., 1995) (Figure 1A). Other behaviors, such as proboscis extension in response to sucrose and circadian rhythms (see Experimental Procedures), were normal in NP5270 > Tnt males, suggesting that the timing phenotype is specific for copulation duration. Moreover, sexual behaviors were not generally aberrant in NP5270 > Tnt males, as they successfully courted females and initiated copulation with normal latency. The copulation postures and dismounting of all animals scored in this study also appeared normal (Figure 1B). This is in contrast to the "stuck" phenotype (Hall, 1981) in which the male dismounts the female and struggles for hours to disengage his genitalia. That the males in this study remained mounted on the female throughout the entirety of the extended copulations, and that copulations terminated without struggle, indicate that the phenotypes do not result from defects in disengagement of genitalia.

We examined the consequences of activating NP5270 neurons by expressing the heat-sensitive *Drosophila* cation channel TrpA1 (Hamada et al., 2008) in NP5270 cells and assaying copulation duration with or without a shift to the activating temperature (30°C). TrpA1 is activated within seconds in response to a temperature shift and is resistant to spike frequency adaptation (Pulver et al., 2009). Although mating durations of control males decreased slightly at 30°C, temperature-shifted NP5270 > TrpA1 males showed a dramatic decrease in copulation duration to 4.8 ± 0.8 min (Figure 1C). We conclude that the activity of NP5270 neurons is a central determinant of copulation duration.

To identify the location of these copulation duration neurons, we examined the expression of membrane-targeted GFP (CD8-GFP) driven by NP5270-Gal4. Within the central nervous system, NP5270 > GFP is detected in small numbers of neurons and in glial cells that ensheath the brain and ventral nerve cord (VNC) (Figure 1D, left). To subtract the glial component of the NP5270 expression pattern, we introduced a RepoGal80 transgene (Awasaki et al., 2008), which selectively inhibits the activity of Gal4 in glia (Figure 1D, center). RepoGal80 had no effect on the copulation duration phenotype of NP5270 > Tnt animals (Figure 1E). In contrast, a pan-neuronal Gal80 transgene, ElavGal80 (Yang et al., 2009), completely suppressed the copulation duration phenotype (Figure 1E), demonstrating that the NP5270 copulation duration cells are neurons.

NP5270 expression in the central nervous system is sparse, with small groups of neurons clustered in several regions of the brain and VNC (Figure 1D). To ask whether NP5270 copulation neurons reside in the brain or VNC, we used a TshGal80 transgene (Clyne and Miesenböck, 2008) to suppress Gal4 activity in the VNC. NP5270 > CD8-GFP, TshGal80 animals retained GFP expression in the brain but lost expression in the VNC (Figure 1D, right). These animals showed no copulation duration phenotype with Tnt (Figure 1E), strongly suggesting that VNC and not brain neurons control copulation timing. To test this, we decapitated wild-type Berlin males within ~3 min after copulation initiation (Figures 1F and 1G). Copulations with headless males terminated only slightly later than those with mock decapitated males (Figure 1G). These results are reminiscent of classic work on mating behavior of the decapitated male praying mantis (Roeder, 1935) and similar results have previously been described in the fly (Tayler et al., 2012). We conclude that neurons in the VNC control copulation timing and that a critical subset of these neurons is marked by the NP5270 Gal4 line.

Uncoupling the Copulation Duration Function of NP5270 Neurons from Fertility

Variation in copulation duration between animal species likely reflects species-specific timing requirements for optimal sperm and accessory factor transfer. To ask whether the circuit that times copulation duration in *Drosophila melanogaster* directly measures the transfer of sperm or male accessory gland fluids, we examined copulation duration in males with impaired fertility. It has been shown (Lefevre and Jonsson, 1962; Linklater et al., 2007), and we confirm, that male fertility declines drastically after approximately three successive matings (Figure 2A, second green bar). However, these reproductively depleted males mate for the same duration as their fully fertile siblings (Figure 2A; compare the two left bars). Moreover, son-of-*tudor* males that lack germ cells and are therefore spermless (Xue and Noll, 2000) showed normal copulation duration (Figure 2A). Males that are missing the primary seminal fluid-producing organs, the accessory glands (via partial rescue of the *paired* mutation) (Bertuccioli et al., 1996; Xue and Noll, 2000), also have no copulation duration phenotype (Figure 2A). These results argue that mating time is not determined directly by the volume or rate of transfer of reproductive fluids.

(C) Temperature-shift copulation duration measured with NP5270 > TrpA1 and parental control males (***$p < 0.001$ indicates a significant interaction term in a two-way ANOVA testing the effects of temperature and genotype; mean ± SEM, n = 12–20).

(D) Immunofluorescence of GFP (green) and nc82 (neuropil, magenta) in the brain (top) and ventral nerve cord (VNC; bottom) of males of the indicated genotypes. Scale bars represent 20 μm.

(E) Copulation duration of NP5270 > Tnt when Tnt expression is suppressed in glia, neurons, or VNC by three Gal80 transgenes (one-way ANOVA and Tukey posttest; genotypes labeled with different letters are statistically different, $p < 0.001$; mean ± SEM, n = 10–11). Red cartoons of brain/VNC below the figure indicate with black shading where Gal4 has been inactivated by Gal80: neurons (inside) and glia (outside) of the brain (top) and VNC (bottom).

(F) Video stills of matings in which wild-type Berlin males were mock decapitated (top) or decapitated (bottom) shortly after copulation initiation.

(G) Copulation durations of matings with mock decapitated or decapitated males as in (F). (**$p < 0.01$, t test; mean ± SEM, n = 15–18). Still photo depicts a decapitated and mock decapitated male mating.

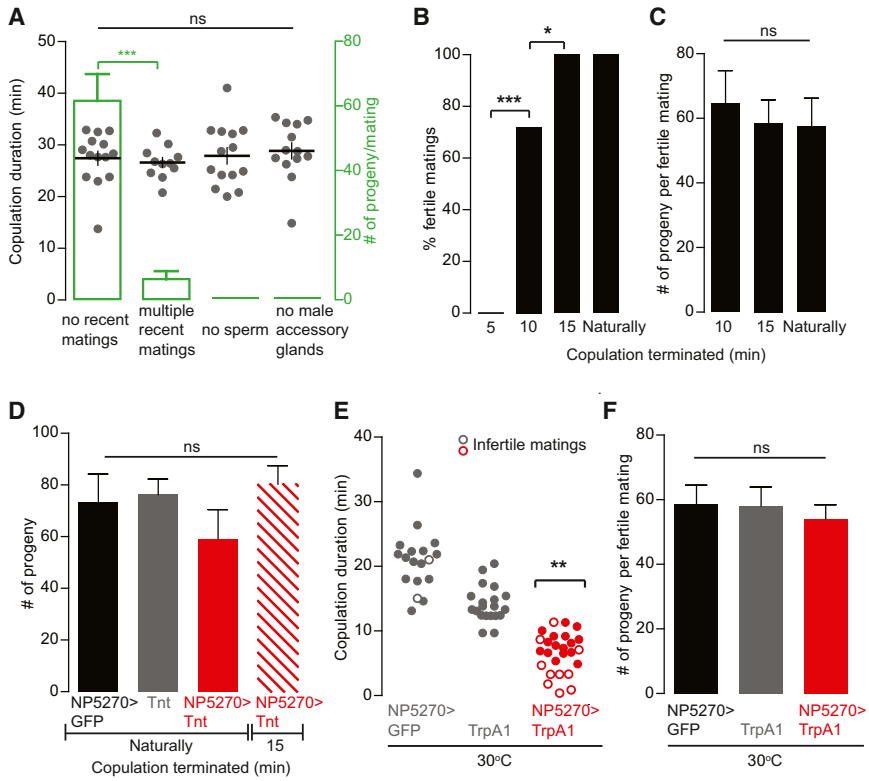

Figure 2. NP5270 Neurons Set Copulation Duration to Allow Time for Reproduction

(A) Copulation duration (gray dots) and fertility (green bars) of wild-type Berlin females with wild-type Berlin males secluded from females for 3 days, or after three to six serial matings; spermless son-of-*tudor* males (Xue and Noll, 2000); and partially rescued *paired* mutant males (Bertuccioli et al., 1996; Xue and Noll, 2000) that lack accessory glands. Copulation duration: ns, not significant, one-way ANOVA; mean ± SEM, n = 13–20. Fertility: ***p < 0.001, t test; mean ± SEM, n = 10–27.

(B and C) Fertile matings (B) and number of progeny per fertile mating (C) resulting from copulation of wild-type Berlin females and NP5270 > CD8-GFP males disrupted at 5, 10, and 15 min after initiation or allowed to terminate naturally. (B) ***p < 0.001, *p < 0.05, overall chi-square test followed by Fisher's exact test for pairs; n = 15–25. (C) ns, not significant, one-way ANOVA; mean ± SEM, n = 15–18.

(D) Number of progeny per mating of wild-type Berlin females with males of the indicated genotype allowed to terminate copulation naturally or disrupted at 15 min (ns, not significant, one-way ANOVA; mean ± SEM, n = 7–10).

(E) Copulation durations of NP5270 > TrpA1 and control males paired with wild-type Berlin females at 30°C. Open dots indicate matings that produced no progeny (**p < 0.01, t test for copulation durations of fertile versus infertile matings of NP5270 > TrpA1 males; mean ± SEM, n = 18–27).

(F) Number of progeny per fertile mating resulting from copulations of the genotypes and conditions shown in (E). ns, not significant, one-way ANOVA; mean ± SEM, n = 26–40.

Experimental disruptions of copulation have shown that full fertilization in laboratory conditions is achieved by ~8 min into copulation (Gilchrist and Partridge, 2000). We confirmed these findings by mechanically separating copulating pairs at various times into copulation. When mating was truncated at 5 min into copulation, females never produced progeny. When matings were disrupted later in copulation, they were usually productive when disrupted at 10 min and always productive when disrupted at 15 min (Figure 2B). Moreover, when these disrupted matings were productive, they produced the same number of progeny as females for which copulation terminated naturally (Figure 2C).

We next asked whether there was any difference in the rate or efficiency of the reproductive process in long-mating NP5270 > Tnt males. The extended matings of NP5270 > Tnt males were fertile and produced the same number of progeny as controls (Figure 2D). To ask whether the fertilization process is delayed in NP5270 > Tnt long-duration matings, we mechanically disrupted copulation of these animals 15 min after initiation. These copulations were fully fertile (Figure 2D). In contrast, copulations with short mating NP5270 > TrpA1 males were often infertile (open circles, Figure 2E). However, when these short matings were fertile, they were as productive as control matings (Figure 2F). Therefore, these copulation duration neurons do not control sperm and seminal fluid transfer, instead they allow sufficient time in copulation for these processes to occur.

NP5270 Neurons Promote a Decline in Copulation Persistence over Time

Because the last ~15 min of copulation seem to be less important for fertility than the first ~10 min, we asked whether the drive to remain in copulation diminishes as copulation progresses. During mating, the male is positioned on top of the female and is unable to escape stressful or dangerous circumstances without terminating copulation. To assay the persistence of copulation, we stressed copulating flies with heat shock by submerging the vial for 30 s in a water bath set to one of three different temperatures, 41°C, 37°C, or 23°C. These heat shocks, if sustained, incapacitate flies at different rates (41°C: 50% incapacitation at 3.2 min; 37°C: 50% incapacitation at 64.6 min; 23°C did not incapacitate flies; Figure 3A). Wild-type pairs almost never separated when heat shocked at any of the three temperatures after copulating for only 5 min (Figure 3B). However, pairs that had been copulating for 10 or more minutes truncated copulations in response to heat shock. The propensity to truncate copulation increased with increasing time into copulation as well as with increasing temperature of heat shock (Figure 3B). Toward the end of copulation, even the 23°C handling control disrupted most copulations. NP5270 > Tnt males did not truncate copulations in response to 41°C heat shock for at least 90 min into mating (Figure 3C), although their avoidance of 41°C when not copulating was as robust as in control males (Figure 3D). These results suggest that a decline in the persistence

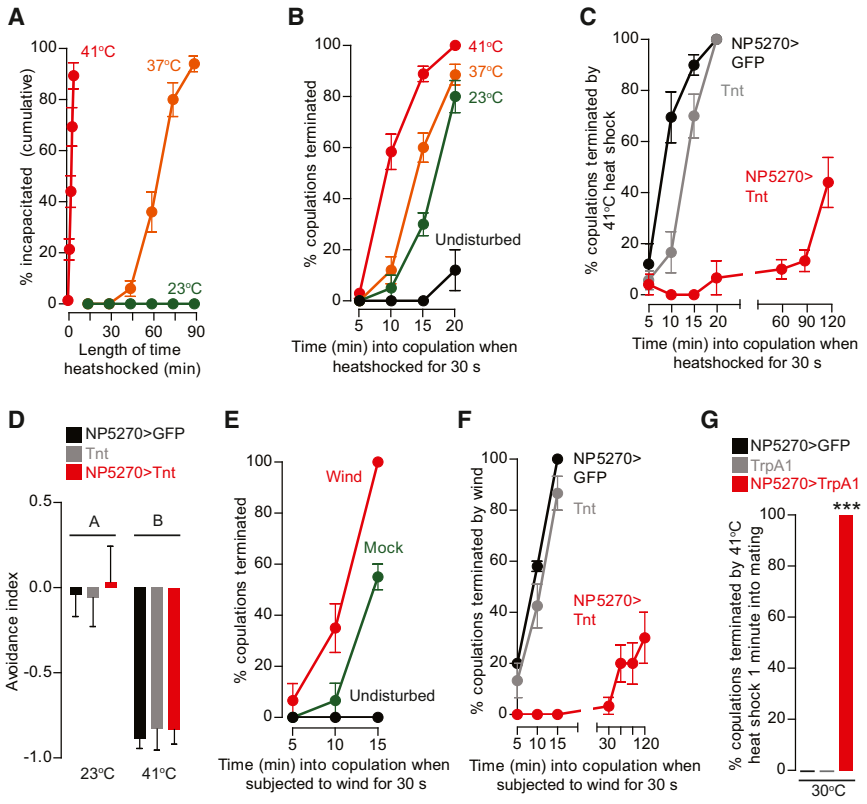

Figure 3. Copulation Timing Neurons Promote a Decline in the Persistence of Copulation

(A) Incapacitation rates of males when subjected to sustained heat shocks of 41°C, 37°C, and 23°C (mean ± SEM, n = 5–15 groups of five).

(B) Copulation termination of wild-type Berlin male and w^{1118} female pairs in response to 30 s 41°C, 37°C, and 23°C heat shocks as well as pairs that were left undisturbed (mean ± SEM, n = 4–19 groups of at least five copulating pairs).

(C) Copulation termination of w^{1118} females and males of the indicated genotypes in response to a 30 s 41°C heat shock (mean ± SEM, n = 3–10 groups of at least five copulating pairs).

(D) Heat avoidance assay (one-way ANOVA and Tukey posttest; genotypes labeled with different letters are statistically different, $p < 0.001$; mean ± SEM, n = 10–11 groups of eight males).

(E) Copulation termination of wild-type Berlin male and w^{1118} female pairs when subjected to 30 s of simulated wind, handling that served as a mock control, or were left undisturbed (mean ± SEM, n = 3–4 groups of at least five copulating pairs).

(F) Copulation termination of w^{1118} females and males of the indicated genotypes in response to 30 s of simulated wind (mean ± SEM, n = 3–6 groups of at least five copulating pairs).

(G) Copulation termination of w^{1118} females and males of the indicated genotypes at 30°C in response to a 30 s 41°C heat shock (***$p < 0.001$, one-way ANOVA with Tukey posttest; mean ± SEM, n = 3 groups of five copulating pairs).

of mating as copulation progresses is promoted by NP5270 neurons.

To challenge copulating pairs with a different sensory stimulus, we subjected them to 30 s of 6.3 ± 0.3 km/hr simulated wind introduced into the vial during copulation. This magnitude of simulated wind is classified as a "light breeze" on the Beaufort wind force scale (Met Office, 2010) and was often sufficient to knock over copulating pairs. Consistent with the heat shock results, pairs that had copulated for 5 min rarely separated in response to simulated wind, whereas all pairs separated when subjected to the wind 15 min into copulation (Figure 3E). Similar to the heat shock experiments, even the mock handling control caused moderate levels of mating disruption at 15 min into copulation (Figure 3E). Again similar to the heat shock data, synaptic silencing of NP5270 neurons prevented wind- and handling-induced copulation disruption at times far beyond those required for optimal sperm and seminal fluid transfer (Figure 3F). Importantly, none of these treatments caused the "stuck" mating phenotype (Hall, 1981) indicating that dismounting and disengaging the genitalia are coordinated outputs of a copulation truncation program.

Having shown that the activity of NP5270 neurons is necessary for the timely reduction in the persistence-like state of the male during copulation, we asked if stimulating these neurons via TrpA1 activation could induce a low-persistence state. A 41°C heat shock applied just 1 min into copulation terminated all copulations in which NP5270 neurons were synthetically activated (Figure 3G). As expected, none of these truncated copulations produced any progeny (data not shown). These results demonstrate that the activity of NP5270 neurons is necessary and sufficient to cause the reduction in persistence that occurs during copulation.

Sexually Dimorphic, GABAergic Interneurons of the Abdominal Ganglion Control Copulation Persistence

NP5270 is an insertion of a Gal4-bearing P-element ~400 bp upstream of the proximal transcription start site of CG17646 (CG17646-RA), which encodes a homolog of the mammalian ABCG1 transporter (Buchmann et al., 2007). This region harbors dozens of P element insertions in various stock collections, including five additional Gal4 insertions from the same collection as NP5270 (Figure 4A). We crossed each of these five Gal4 insertions to UAS-Tnt and observed significant copulation lengthening in every case (Figure 4B). We analyzed the expression pattern and behavioral phenotype of NP2719 in greater detail because it had the sparsest VNC expression of all six Gal4 lines (Figure 4C).

NP2719 > CD8-GFP showed selective expression in ~12 cells in the distal segment of the VNC, the abdominal ganglion (Figures 4C, 5A, and 5B). NP2719 neurons appear to arborize throughout the abdominal ganglion (Figure 5A). NP2719 expression was not detected in neurons innervating the reproductive organs (data not shown). When we used NP2719 to drive expression of GFP targeted to synaptic vesicles (nsyb-GFP) (Estes et al., 2000), we observed presumptive presynaptic termini throughout the abdominal ganglion (Figure 5C),

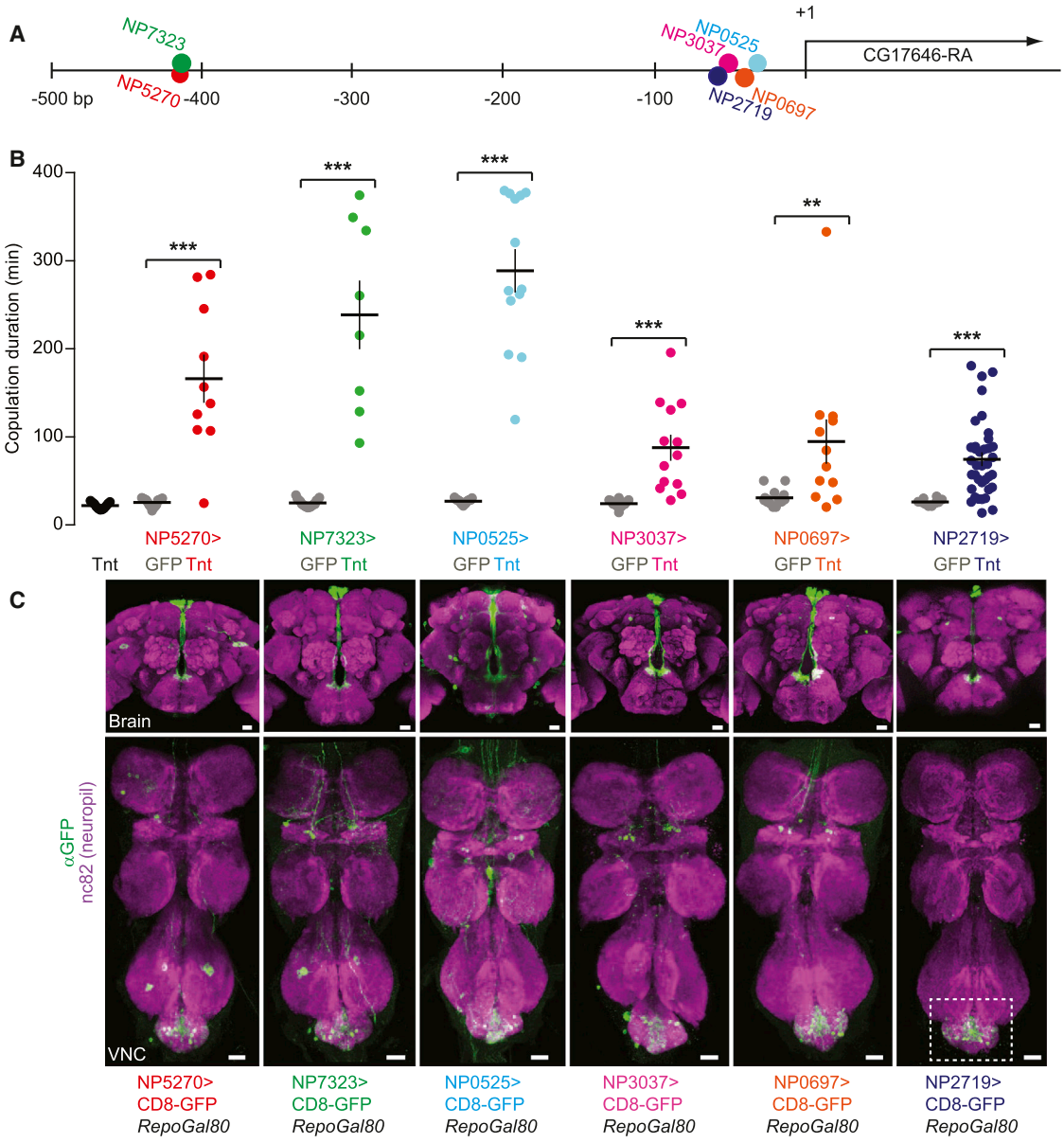

Figure 4. Abdominal Ganglion Interneurons Time Copulation

(A) Schematic of the *CG17646-RA* locus with Gal4 insertions marked by colored dots.

(B) Copulation duration of six Gal4 lines crossed to UAS-CD8-GFP (gray) or UAS-Tnt (colors) compared to UAS-Tnt/+ (black) without Gal4 for reference (**p < 0.01, ***p < 0.001, t test to assess differences between experimental and control genotypes for each Gal4 line; mean ± SEM, n = 8–37).

(C) Immunofluorescence of GFP (green) and nc82 (neuropil, magenta) in brains (top) and VNCs (bottom) of males of the indicated genotypes. The abdominal ganglion is indicated by the dashed box at the far right. Scale bars represent 20 μm.

suggesting that the NP2719-expressing cells are abdominal ganglion interneurons. When we activated the NP2719 neurons with TrpA1, copulation duration was significantly shortened (Figure 5D). Thus, these ~12 neurons represent a compact subset of the neurons whose activity determines the duration of copulation.

To identify the molecules through which these interneurons communicate information about copulation duration, we used NP5270-Gal4 and NP2719-Gal4 to drive UAS-RNAi transgenes directed against components of the major neurotransmitter systems of the fly. Of all the lines screened, only RNAi knockdown of *Glutamic acid decarboxylase 1* (*Gad1*) or *Vesicular GABA transporter* (*VGAT*) phenocopied the effects of silencing the neurons with Tnt (Figure 5E). *Gad1* encodes the enzyme that synthesizes the inhibitory neurotransmitter γ-aminobutyric acid (GABA) and *VGAT* packages GABA into synaptic vesicles. Staining for GABA showed colocalization with the cell bodies of 70% ± 6% or ~8 of the 12 NP2719-Gal4 abdominal ganglion neurons

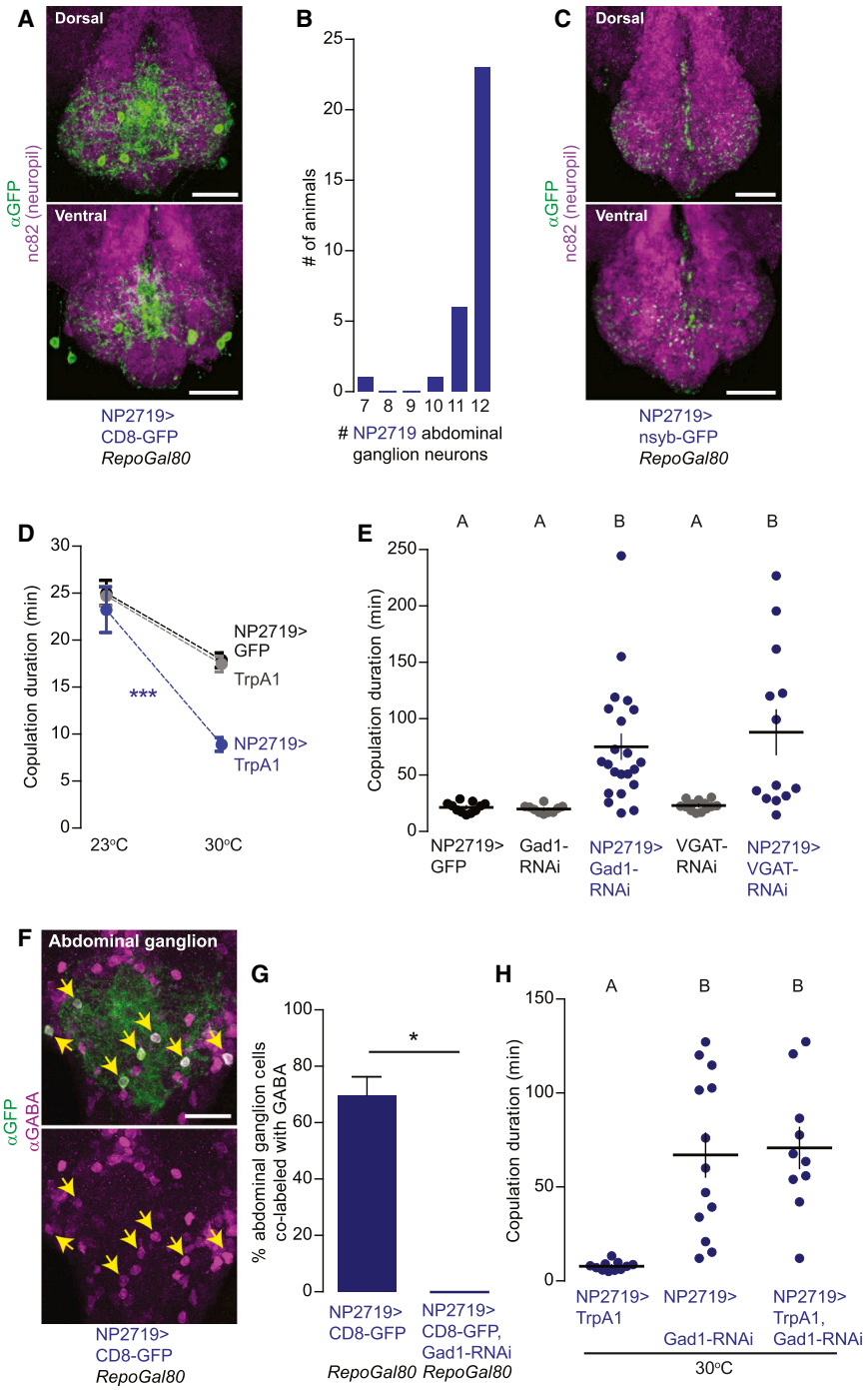

Figure 5. Abdominal Ganglion Timing Interneurons Are GABAergic

(A) Immunostaining of GFP (green) and nc82 (neuropil, magenta) in NP2719 > CD8-GFP, RepoGal80 male abdominal ganglia. Scale bars represent 20 μm.

(B) Histogram of number of GFP-positive cells in abdominal ganglia of NP2719 > CD8-GFP, RepoGal80 males (n = 31).

(C) Immunostaining of GFP (green) and nc82 (neuropil, magenta) in abdominal ganglia of NP2719 > nsyb-GFP, RepoGal80 males. Scale bars represent 20 μm.

(D) Copulation durations measured at 23°C and 30°C using males of the indicated genotypes (***$p < 0.001$, indicates a significant interaction term in a two-way ANOVA testing the effects of temperature and genotype; mean ± SEM, n = 10–12).

(E) Copulation durations of males with RNAi knockdown of GABA components in NP2719-Gal4 neurons compared to controls (one-way ANOVA and Tukey posttest; genotypes labeled with different letters are statistically different, $p < 0.05$; mean ± SEM, n = 10–22).

(F) Immunostaining of GFP (green) and GABA (magenta) in NP2719 > CD8-GFP, RepoGal80 male abdominal ganglia. Yellow arrows point to cell bodies of neurons colabeling for NP2719 and GABA. Scale bar represents 20 μm.

(G) Quantification of NP2719 > CD8-GFP, RepoGal80 abdominal ganglion cells with coexpression of GFP and GABA (*$p < 0.05$, Mann-Whitney test; mean ± SEM, n = 3–8 animals; 29–56 cells examined in total).

(H) Copulation durations of males with NP2719 neurons activated by TrpA1, RNAi knockdown of Gad1 in NP2719 neurons, and NP2719 neurons activated in combination with RNAi knockdown of Gad1. (one-way ANOVA and Tukey posttest; genotypes labeled with different letters are statistically different, $p < 0.001$; mean ± SEM, n = 11–13).

inal ganglion interneurons is a critical determinant of copulation duration and persistence.

Unlike in other species of flies (Mazzi et al., 2009), in *Drosophila melanogaster* copulation duration is controlled by the male (Acebes et al., 2004; Beaver and Giebultowicz, 2004; Lee et al., 2001; MacBean and Parsons, 1967), with little influence of the female. To ask whether the identified GABAergic neurons were sexually dimorphic, we examined the expression of NP5270 and NP2719 in females. Although brain and thoracic ganglion expression of these lines was similar in males and females, expression was not detected in female abdominal ganglion neurons (Figures 6A and 6B; data not shown).

To explore the molecular basis of this sexual dimorphism, we examined the expression of Fruitless (Fru) and Doublesex (Dsx) in NP2719 abdominal ganglion neurons. *fru* and *dsx*

(Figures 5F and 6G). GABA immunoreactivity in NP2719 neurons was abolished in NP2719 > Gad1-RNAi animals, indicating that our RNAi was effective (Figure 5G). GABA is likely the sole effector of copulation duration released by these neurons because stimulating NP2719 neurons via TrpA1 activation while knocking down Gad1 resulted in long copulations (Figure 5H). Similar results were obtained using NP5270-Gal4 (data not shown). Thus GABA release from ~8 male-specific abdom-

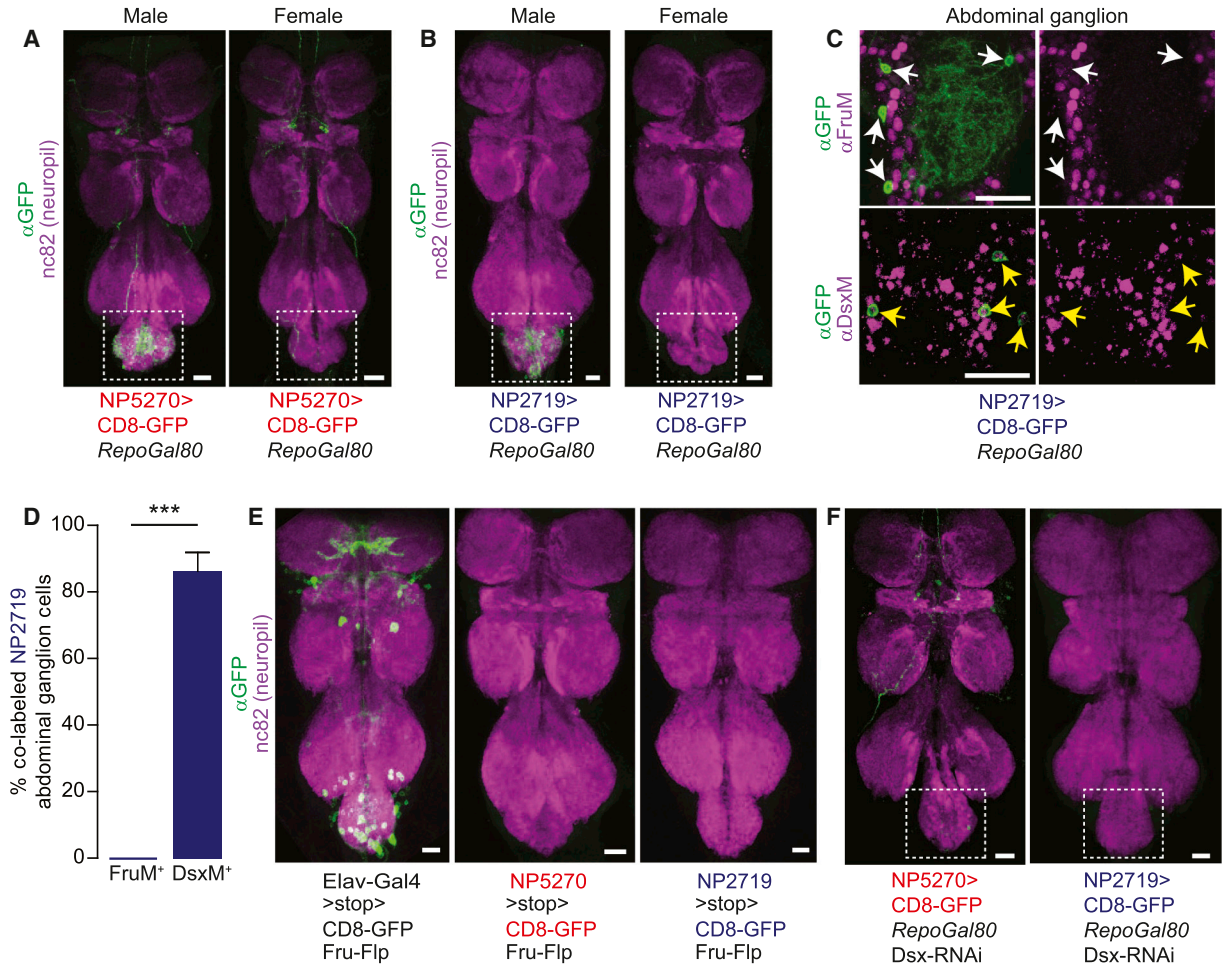

Figure 6. The GABAergic Interneurons Are Sexually Dimorphic

(A and B) Immunofluorescence of GFP (green) and nc82 (neuropil, magenta) in VNCs of male and female (A) NP5270 > CD8-GFP, RepoGal80 and (B) NP2719 > CD8-GFP, RepoGal80 animals.

(C) Immunofluorescence of GFP (green) and FruM (top, magenta) or DsxM (bottom, magenta) in abdominal ganglia of male NP2719 > CD8-GFP, RepoGal80 animals. White arrows point to NP2719 cell bodies that do not colabel with FruM, yellow arrows point to NP2719 cell bodies that colabel with DsxM.

(D) Quantification of NP2719 > CD8-GFP, RepoGal80 abdominal ganglion cells with coexpression of GFP and FruM or DsxM (***$p < 0.001$, Mann-Whitney test; mean ± SEM, n = 7–8 animals; 35–41 cells examined in total).

(E) Immunofluorescence of GFP (green) and nc82 (neuropil, magenta) in male VNCs in which Fru-Flp has been used to excise a stop cassette preventing expression of CD8-GFP when driven by (left) Elav-Gal4, (center) NP5270-Gal4, or (right) NP2719-Gal4.

(F) Immunofluorescence of GFP (green) and nc82 (neuropil, magenta) in the VNC of NP5270 > CD8-GFP, RepoGal80 (left) and NP5270 > CD8-GFP, RepoGal80 (right) males also expressing UAS-Dsx-RNAi. In (A), (B), and (F) abdominal ganglia are indicated by white dashed boxes. Scale bars represent 20 μm.

are transcription factors that are spliced into male- and female-specific isoforms by sex-specific splicing factors (Dickson, 2008; Rideout et al., 2010) that instruct morphological and behavioral dimorphisms in the fly. Double labeling of male NP2719 > CD8-GFP neurons with antibodies raised against male-specific isoforms of these proteins (FruM or DsxM) revealed that the majority were labeled with anti-DsxM, whereas none were stained by anti-FruM (Figures 6C and 6D). Moreover, none of the NP5270 or NP2719 VNC neurons were labeled by Fru-Flp (Yu et al., 2010) (Figure 6E), arguing that they did not express *fru* at any point during development. Finally, when we targeted *dsx* with an RNAi transgene under the control of NP5270-Gal4 or NP2719-Gal4, the sexually dimorphic abdominal ganglion expression was lost (Figure 6F). We conclude that *dsx* instructs sexual dimorphism in these neurons.

Dopaminergic Neurons Sustain Copulation

Dopamine signaling has been implicated in various motivated behaviors in species as diverse as insects and humans (Perry and Barron, 2013; Wise, 2004). Having shown that copulation duration is a product of declining persistence, we hypothesized a role for dopamine signaling in copulation duration. We stimulated dopaminergic neurons by driving TrpA1 expression with Gal4 under the control of the *cis*-regulatory DNA of *pale*, which encodes tyrosine hydroxylase, the rate-limiting enzyme in

dopamine synthesis (TH-Gal4) (Friggi-Grelin et al., 2003). Activating TH-Gal4 neurons in males dramatically extended copulation duration (Figure 7A), but did not noticeably affect fertility or lead to "stuck" phenotypes. This extension of copulation duration was associated with a lengthening of the period of high-persistence copulation (Figure 7B), demonstrating that dopamine signaling promotes copulation persistence. TshGal80 largely suppressed TH-Gal4 activity in the VNC (Figure 7C), whereas Gal4 activity in the brain was not noticeably affected (data not shown). TshGal80 suppressed the ability of TH-Gal4 neurons to extend copulation duration when stimulated by TrpA1 activation (Figure 7D), indicating that the dopaminergic neurons controlling copulation duration reside in the VNC.

Our attempts to silence TH-Gal4 neurons or to block dopamine processing led either to lethality or to a suppression of sexual behavior, preventing an assessment of copulation duration. Instead, we examined mutations in the four reported *Drosophila* dopamine receptors. Surprisingly, loss-of-function mutations in all four dopamine receptors resulted in reduced copulation duration relative to genetic background controls (Figures 7E–7H). A deletion mutation in *DopR1* (Keleman et al., 2012) and a transposable element insertion into *DopEcR* (Inagaki et al., 2012) resulted in particularly strong reductions in copulation duration (Figures 7E and 7F). These results argue that dopaminergic neurons signal through multiple dopamine receptors to sustain copulation.

The GABAergic neurons of the abdominal ganglion and the dopaminergic neurons of the VNC work in opposition to determine copulation persistence and, thereby, copulation duration. To assess the relative influence of the GABAergic and dopaminergic populations we simultaneously stimulated them via TrpA1 activation. Stimulation of the GABAergic neurons largely suppressed the ability of dopaminergic neurons to extend copulation (Figure 7I). Similar results were seen with NP5270-Gal4 (data not shown). This suppression may take place in the abdominal ganglion, where GABAergic and dopaminergic neurons are intermingled (Figure 7J).

DISCUSSION

Some behaviors are reflexive, occurring in specific circumstances regardless of internal states or competing external stimuli. In contrast, many behaviors are influenced by motivational processes, of which there are three main classes: selection, intensity, and persistence (Carlson et al., 2007). Although the extent to which terms from human psychology such as "motivation" and "persistence" are appropriate for insects is unclear, we show that male *Drosophila* display flexible, persistence-like behavior in determining whether or not to terminate copulation given the conditions internal and external to the animal.

The GABAergic and dopaminergic neurons that we have identified work in opposition to set copulation duration by changing the behavioral state of the male fly over time. Neither population has any demonstrable control over the transfer of reproductive fluids. Previously reported populations of neurons in the male abdominal ganglion control copulation duration as well as reproductive fluid transfer (Acebes et al., 2004; Lee et al., 2001; Tayler et al., 2012), although Tayler et al. (2012) experimentally dissociated the control of copulation duration and reproductive fluid transfer. The neurons studied here also differ from known populations of copulation neurons because their sexual dimorphism is instructed by *dsx* and not *fru*. Thus there are several functionally, anatomically, and molecularly distinct neuronal inputs into copulation duration in the fly.

Some neurons that influence copulation duration supply information regarding relevant internal and external circumstances. For example, in addition to the in copulo flexibility we document here, mating time in *Drosophila* has been shown to increase ~10%–20% if the male is housed in the presence of "competitor" males (Kim et al., 2012; Wigby et al., 2009), changes modestly within the first 3 days of male adulthood, is extended in *period* and *timeless* circadian rhythm mutants (Beaver and Giebultowicz, 2004), and is subject to alteration by artificial selection (MacBean and Parsons, 1967). Thus copulation persistence may emerge from interactions between neuronal populations carrying information about internal states and life history, as well as about the progress of copulation. Our data suggest a role for the GABAergic interneurons as a central node in this circuitry that integrates information from these inputs to produce a cohesive behavioral state that changes as copulation progresses.

The decline in copulation persistence proceeds as the probability that the mating has been successful increases. Under adverse conditions such as the heat or wind used here, persistence provides an important component of a cost-benefit analysis that determines whether or not to truncate the copulation. We propose that GABA release causes persistence to decline until it reaches a threshold at which other internal drives or opportunities are sufficient to reorient the male toward other behavioral goals. These GABAergic interneurons may operate over a relatively broad dynamic range, contributing both to copulation duration under calm conditions but also instructing premature copulation in the face of stressful external conditions.

Although the decline in copulation persistence occurs on a timescale that ensures productive mating, it appears to be regulated by an interval timing mechanism independent of reproductive fluid transfer. This raises the possibility that a long-sought mechanism for neural interval timing may be found by further study of this simple behavior. The involvement of conserved neurotransmission systems increases our confidence that copulation duration is a useful model for investigating the poorly understood phenomena of interval timing and persistence.

EXPERIMENTAL PROCEDURES

Fly Stocks

Flies were maintained on conventional cornmeal-agar-molasses medium under a 12 hr light:12 hr dark (9 a.m.–9 p.m.) cycle at 25°C and ambient humidity. Males were collected 0–3 days after eclosion and were group housed away from females for 3–13 days. Virgin females were group housed and were 3–13 days old when used. Detailed genotypes of all strains used in the paper are listed in the Extended Experimental Procedures available online.

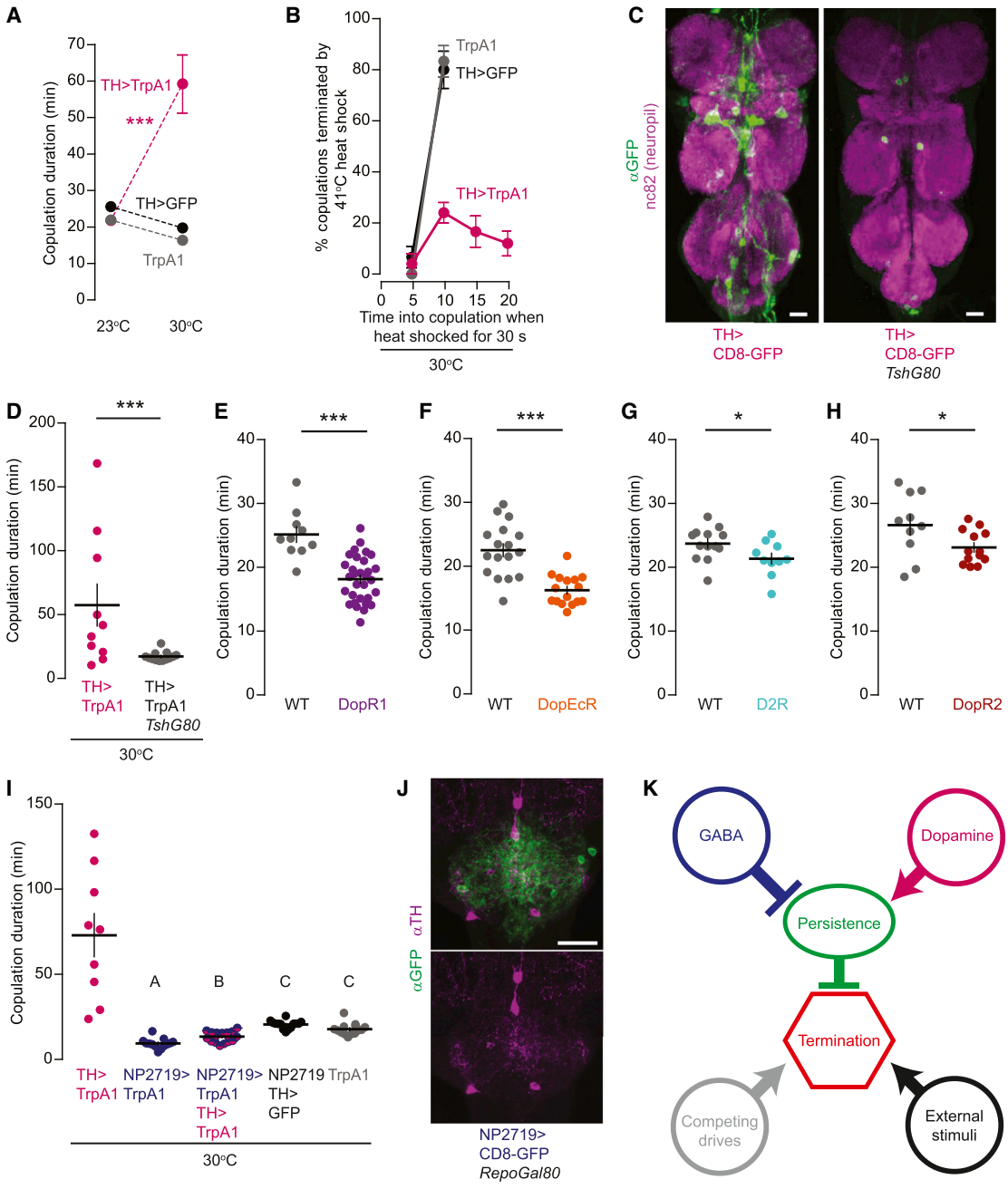

Figure 7. Dopaminergic VNC Neurons Sustain Copulation

(A) Copulation durations measured at 23°C and 30°C using TH > TrpA1 and parental control males (***$p < 0.001$ indicates a significant interaction term in a two-way ANOVA testing the effects of temperature and genotype; mean ± SEM, n = 9–23).

(B) Copulation termination of w^{1118} females and males of the indicated genotypes at 30°C in response to a 30 s 41°C heat shock (mean ± SEM, n = 5–6 groups of five copulating pairs).

(C) Immunofluorescence of GFP (green) and nc82 (neuropil, magenta) VNC of males of the indicated genotypes. Scale bars represent 20 μm.

(D) Copulation durations of TH > TrpA1 males at 30°C with and without suppression of TrpA1 expression in the VNC by TshGal80 (***$p < 0.001$, t test; mean ± SEM, n = 10–13).

(E–H) Copulation durations of males mutant for the dopamine receptors *DopR1* (E), *DopEcR* (F), *D2R* (G), and *DopR2* (H) compared to their wild-type background strains (***$p < 0.001$, *$p < 0.05$ t test; mean ± SEM, n = 10–31).

(I) Copulation durations of males of the indicated genotypes at 30°C (genotypes labeled with different letters are statistically different, one-way ANOVA and Tukey posttest excluding the TH > TrpA1 genotype, $p < 0.01$; mean ± SEM, n = 9–17).

(J) Immunofluorescence of GFP (green) and TH (magenta) in the abdominal ganglion of a NP2719 > CD8-GFP RepoGal80 male. Scale bar represents 20 μm.

(K) Schematic of the relationships between several determinants of copulation duration.

Screen for Hypersexual Males

The NP5270-Gal4 line was identified in a screen for males that spend more time in copulation than wild-type males. Individual males were placed in a food vial with 20 w^{1118} virgin females and copulation was monitored 3 hr later. NP5270 > Tnt animals were discovered after screening ~2,500 lines with various genetic perturbations that were not reproducibly scored as hypersexual in this assay.

Fertility Experiments

Wild-type Berlin females 3–13 days of age were used for fertility experiments. Detailed genotypes of males used for fertility experiments are in the Extended Experimental Procedures. Immediately after mating, the female was isolated in a food vial at 25°C. After 7 days, the female was removed from the vial and adult progeny were scored 10 days later. All males were separated from females at 0–3 days posteclosion and were group-housed for 3–13 days. Males classified as having had "multiple recent matings" were previously paired with 30 virgin w^{1118} females for 4.5 hr. During this time males mated an average of three to six times (data not shown), drastically reducing their fertility upon subsequent copulation (Lefevre and Jonsson, 1962; Linklater et al., 2007).

Mechanical Copulation Disruption

Copulation of a single pair was disrupted mechanically with a paintbrush. A paintbrush (size 1, tip size 1/32") was placed between the male and female along their abdominal contact surface while they were copulating inside the food vial in which they were mating. The brush was moved back and forth to separate the animals, an operation that took between <1 s to ~5 s depending on the particular pair and how long they had been in copulation.

Behavioral Assays

Copulation Duration Assays

Standard copulation duration assays took place at room temperature (22°C –24°C) and ambient humidity from 10 a.m.–6 p.m. Each trial consisted of 15 polystyrene fly vials (28.5 mm × 95 mm, Applied Scientific) containing standard *Drosophila* food and plugged with a standard Buzz Plug (Applied Scientific) that had been cut at an angle to allow video scoring. Each vial contained a single male and two virgin females. Males of various genotypes were aged 3–13 days and isolated from females for at least 3 days. Groups of up to 18 vials were videotaped using a consumer grade high definition digital camcorder (Canon Vixia HFR20 HD) for at least 1 hr or until all copulation had ceased and manually scored using Media Player Classic (v. 1.5.3.3752 for Windows; SourceForge, http://mpc-hc.sourceforge.net/) for the duration of the first copulation. Temperature-shifted copulation duration assays were videotaped inside a 30°C incubator. The copulation shown in Figure 1C was videotaped in a courtship chamber of 1 cm diameter and 3 mm depth with 1% agarose gel on the bottom to provide humidity.

Approximately 20% of copulations that lasted for multiple hours began to exhibit a "stuck" phenotype (Hall, 1981). Any trials in which copulations exhibited the "stuck" phenotype were discarded and their data not used in the analysis of copulation duration.

Mating Latency Assay

Mating latency was measured in standard copulation duration assays. NP5270 > GFP: 6.1 ± 1.4 min, Tnt: 8.2 ± 1.4 min, NP5270 > Tnt: 5.3 ± 1.2 min; not significant, one-way ANOVA; mean ± SEM, n = 14–19.

Decapitated-Male Copulation Duration Assays

Individual pairs of male and virgin female wild-type Berlin flies were visually monitored for copulation initiation, upon which they were immediately aspirated onto a Petri dish coated with petroleum jelly to minimize locomotion of the copulating animals. Microscissors were placed around the neck of the male and clipped (for decapitation) or retracted (for mock decapitation). Male-decapitated and mock-decapitated pairs were then aspirated into a courtship chamber (1 cm diameter, 3 mm depth) and videotaped for the remaining duration of copulation. If the time from copulation initiation to videotaping exceeded 3 min, the pair was discarded. Copulations were only scored if decapitated males were healthy enough to right themselves and groom after copulation termination.

Copulation Disruption Assays

Incapacitation by Heat Shock. To examine the effect of heat shock at different temperatures on male posture and behavior, groups of five wild-type Berlin males were placed in standard fly vials that had not been filled with fly food. An individual vial was submerged in the water bath and removed for few a seconds for visual scoring of the posture of the flies, then replaced into the bath. Animals were scored as incapacitated if they were not in an upright position or failed to respond when the vial was tapped against the side of the water bath. 50% incapacitation times were interpolated from linear (41°C) or nonlinear (37°C) curve fitting. Animals heat shocked at 41°C were scored every minute for 5 min. Animals heat shocked at 37°C or 23°C were scored every 15 min for 90 min.

Heat Shock during Copulation. Groups of approximately ten males were placed with approximately ten virgin w^{1118} females in standard fly food vials and monitored for copulation at ambient temperature and humidity. Upon initiation of copulation, a mating pair was aspirated into a standard fly vial that had not been filled with fly food. At the indicated time into copulation, the vial containing the copulating pair was submerged in a 41°C, 37°C, or 23°C water bath for 30 s. After the 30 s heat shock, the vial was removed from the water bath and the copulating pair visually monitored for copulation termination. If the copulation was terminated during the 30 s heat shock or in the ensuing 2 min after removal from the water bath while the vial was held at room temperature, it was scored as terminated by heat shock. Pairs were scored in groups of five. Undisturbed copulations were not touched and were scored for termination every 5 min. Experiments involving stimulation by TrpA1 activation were performed with a water bath set to 41°C inside a 30°C room.

Heat Avoidance Assay. Groups of eight males were aspirated into a 2 ml Costar serological pipette that had its ends sawed off to 15 cm. The pipette was sealed at both ends with Parafilm and inserted into a one-hole rubber stopper (size 5½; VWR CAT#59581-265) so that 6 cm of pipette protruded from either side of the stopper. The stopper was fit snugly into the top of a standard food vial filled with 41°C or 23°C water. The assay was laid on its side for 2 min and the number of animals on the "open" and "water" sides was scored. Animals that were occluded by the rubber stopper were not scored. Avoidance indices were calculated as ([% animals on water side] – [% animals on air side])/100.

Simulated Wind during Copulation. Copulating pairs were prepared as described above for heat shocking except that the food vial was capped with a buzz plug that contained two holes large enough to fit a 200 μl pipette tip. At the indicated time into copulation the vial containing the copulating pair was moved to a test tube rack and a 200 μl pipette tip was inserted through one of the holes in the buzz plug. This pipette tip was connected through airline tubing (Python) to a solenoid valve (Parker, VAC-50-PSIG) that was connected through airline tubing to a quiet vacuum/pressure pump (Cole Parmer, EW-79610-02). The solenoid valve was operated by a custom MATLAB script controlling a valve controller (NResearch, 360D1X75R) through a digital interface (Measurement Computing, USB-1208FS) to direct airflow into the food vial for 30 s. Mating pairs that terminated during the 30 s of simulated wind, or within the ensuing 2 min were scored as disrupted. Pairs were scored in groups of five. Mock pairs were moved to the test tube rack and a 200 μl pipette tip was inserted for 30 s, but it was not connected to the solenoid valve or air pump. Undisturbed copulations were not touched, but were scored for termination every 5 min for 20 min. Air speed was measured with a Velocicalc air velocity meter (TSI, 8345).

Circadian Rhythms

Locomotor activity levels were monitored in a 25°C incubator using the *Drosophila* Activity Monitoring System (Trikinetics). Flies were entrained in 12 hr light:12 hr dark conditions for 5 days before transferring to and scoring in constant darkness. Locomotor counts were collected every minute, binned at 30 min, and analyzed using Clocklab (Actimetrics). 19/20 NP5270 > Tnt flies tested were rhythmic with a period of 23.8 ± 0.1 hr (mean ± SEM).

Proboscis Extension Assay

The wings of males that had been water-fasted for 24 hr were taped to a slide such that the ventral side of the animal was facing up. One microliter of 100 mM sucrose was drawn into a 10 μl pipette tip using a 10 μl pipette and partially expelled from the pipette tip in order to form a bubble. The bubble was presented to the proboscis of the males four to five times and proboscis extension

was recorded as per cent extension for each animal. NP5270 > GFP: 87% ± 5%; TntG: 95% ± 3%; NP5270 > TntG: 86% ± 4%; not significant, one-way ANOVA; mean ± SEM, n = 9–10 animals.

Immunostaining and Microscopy

Samples were prepared essentially as described (Ostrovsky et al., 2010). For details on procedures and antibodies used see the Extended Experimental Procedures.

Statistical Analysis

Statistical analysis was performed using GraphPad Prism Software version 5.04 (GraphPad Software).

SUPPLEMENTAL INFORMATION

Supplemental Information includes Extended Experimental Procedures and can be found with this article online at http://dx.doi.org/10.1016/j.cell.2013.09.055.

AUTHOR CONTRIBUTIONS

M.A.C. designed and carried out all the experiments in the paper. M.A.C. and L.B.V. composed the figures and wrote the paper.

ACKNOWLEDGMENTS

We thank Kevin J. Lee, Gaby Maimon, Alex Nectow, Dragana Rogulja, Vanessa Ruta, and members of the Vosshall Lab for discussion and comments on the manuscript; David Anderson, Barry Dickson, Yuh Nung Jan, Tzumin Lee, Julie Simpson, and Markus Noll for providing fly stocks; Daisuke Yamamoto and Brian Oliver for antibodies; Alison Hill, Sarah Puhr, and Stephen Conway for expert technical assistance; Roman Corfas and Ben Matthews for help with the simulated wind experiments; and Dragana Rogulja and Mike Young for help measuring circadian rhythms. Rachel Zipursky helped initiate experiments with the decapitated males in Figures 1F and 1G. Veronica Burnham helped with heat shock of copulating pairs in Figure 3B. L.B.V. is an investigator of the Howard Hughes Medical Institute. M.A.C. was supported by Marco Stoffel Mind, Brain, and Behavior and Helen Hay Whitney Postdoctoral Fellowships.

Received: April 5, 2013
Revised: August 10, 2013
Accepted: September 24, 2013
Published: November 7, 2013

REFERENCES

Acebes, A., Grosjean, Y., Everaerts, C., and Ferveur, J.F. (2004). Cholinergic control of synchronized seminal emissions in *Drosophila*. Curr. Biol. *14*, 704–710.

Atkinson, J.W., and Birch, D. (1970). The dynamics of action (New York, N.Y.: John Wiley & Sons, Inc.).

Awasaki, T., Lai, S.L., Ito, K., and Lee, T. (2008). Organization and postembryonic development of glial cells in the adult central brain of *Drosophila*. J. Neurosci. *28*, 13742–13753.

Beaver, L.M., and Giebultowicz, J.M. (2004). Regulation of copulation duration by *period* and *timeless* in *Drosophila melanogaster*. Curr. Biol. *14*, 1492–1497.

Bertuccioli, C., Fasano, L., Jun, S., Wang, S., Sheng, G., and Desplan, C. (1996). *In vivo* requirement for the paired domain and homeodomain of the *paired* segmentation gene product. Development *122*, 2673–2685.

Boisvert, M.J., and Sherry, D.F. (2006). Interval timing by an invertebrate, the bumble bee *Bombus impatiens*. Curr. Biol. *16*, 1636–1640.

Brand, A.H., and Perrimon, N. (1993). Targeted gene expression as a means of altering cell fates and generating dominant phenotypes. Development *118*, 401–415.

Buchmann, J., Meyer, C., Neschen, S., Augustin, R., Schmolz, K., Kluge, R., Al-Hasani, H., Jürgens, H., Eulenberg, K., Wehr, R., et al. (2007). Ablation of the cholesterol transporter adenosine triphosphate-binding cassette transporter G1 reduces adipose cell size and protects against diet-induced obesity. Endocrinology *148*, 1561–1573.

Buhusi, C.V., and Meck, W.H. (2005). What makes us tick? Functional and neural mechanisms of interval timing. Nat. Rev. Neurosci. *6*, 755–765.

Carlson, N.R., Heth, C.D., Miller, H., Donahoe, J.W., Buskist, W., and Martin, G.N. (2007). Psychology: The Science of Behavior (Boston: Allyn & Bacon).

Clyne, J.D., and Miesenböck, G. (2008). Sex-specific control and tuning of the pattern generator for courtship song in *Drosophila*. Cell *133*, 354–363.

Dickson, B.J. (2008). Wired for sex: the neurobiology of *Drosophila* mating decisions. Science *322*, 904–909.

Estes, P.S., Ho, G.L., Narayanan, R., and Ramaswami, M. (2000). Synaptic localization and restricted diffusion of a *Drosophila* neuronal synaptobrevin—green fluorescent protein chimera in vivo. J. Neurogenet. *13*, 233–255.

Friggi-Grelin, F., Coulom, H., Meller, M., Gomez, D., Hirsh, J., and Birman, S. (2003). Targeted gene expression in *Drosophila* dopaminergic cells using regulatory sequences from tyrosine hydroxylase. J. Neurobiol. *54*, 618–627.

Gilchrist, A.S., and Partridge, L. (2000). Why it is difficult to model sperm displacement in *Drosophila melanogaster*: the relation between sperm transfer and copulation duration. Evolution *54*, 534–542.

Grant, B.R. (1983). On the relationship between average copulation duration and insemination reaction in the genus *Drosophila*. Evolution *37*, 854–856.

Hall, J.C. (1981). Sex behavior mutants in *Drosophila*. BioScience *31*, 125–130.

Hamada, F.N., Rosenzweig, M., Kang, K., Pulver, S.R., Ghezzi, A., Jegla, T.J., and Garrity, P.A. (2008). An internal thermal sensor controlling temperature preference in *Drosophila*. Nature *454*, 217–220.

Hempel, L.U., and Oliver, B. (2007). Sex-specific DoublesexM expression in subsets of *Drosophila* somatic gonad cells. BMC Dev. Biol. *7*, 113.

Inagaki, H.K., Ben-Tabou de-Leon, S., Wong, A.M., Jagadish, S., Ishimoto, H., Barnea, G., Kitamoto, T., Axel, R., and Anderson, D.J. (2012). Visualizing neuromodulation in vivo: TANGO-mapping of dopamine signaling reveals appetite control of sugar sensing. Cell *148*, 583–595.

Keleman, K., Vrontou, E., Krüttner, S., Yu, J.Y., Kurtovic-Kozaric, A., and Dickson, B.J. (2012). Dopamine neurons modulate pheromone responses in *Drosophila* courtship learning. Nature *489*, 145–149.

Kim, W.J., Jan, L.Y., and Jan, Y.N. (2012). Contribution of visual and circadian neural circuits to memory for prolonged mating induced by rivals. Nat. Neurosci. *15*, 876–883.

Kimura, K., Hachiya, T., Koganezawa, M., Tazawa, T., and Yamamoto, D. (2008). *Fruitless* and *doublesex* coordinate to generate male-specific neurons that can initiate courtship. Neuron *59*, 759–769.

Lee, T., and Luo, L. (1999). Mosaic analysis with a repressible cell marker for studies of gene function in neuronal morphogenesis. Neuron *22*, 451–461.

Lee, G., Villella, A., Taylor, B.J., and Hall, J.C. (2001). New reproductive anomalies in *fruitless*-mutant *Drosophila* males: extreme lengthening of mating durations and infertility correlated with defective serotonergic innervation of reproductive organs. J. Neurobiol. *47*, 121–149.

Lefevre, G., Jr., and Jonsson, U.B. (1962). Sperm transfer, storage, displacement, and utilization in *Drosophila melanogaster*. Genetics *47*, 1719–1736.

Linklater, J.R., Wertheim, B., Wigby, S., and Chapman, T. (2007). Ejaculate depletion patterns evolve in response to experimental manipulation of sex ratio in *Drosophila melanogaster*. Evolution *61*, 2027–2034.

MacBean, I.T., and Parsons, P.A. (1967). Directional selection for duration of copulation in *Drosophila melanogaster*. Genetics *56*, 233–239.

Mazzi, D., Kesäniemi, J., Hoikkala, A., and Klappert, K. (2009). Sexual conflict over the duration of copulation in *Drosophila montana*: why is longer better? BMC Evol. Biol. *9*, 132.

Met Office (2010). Fact sheet 6—The Beaufort Scale. http://www.metoffice.gov.uk/media/pdf/b/7/Fact_sheet_No._6.pdf.

Ostrovsky, A., Cachero, S., and Jefferis, G.S. (2010). Studying olfactory development and neuroanatomy with clonal analysis. In *Drosophila* Neurobiology: A Laboratory Manual, B. Zhang, M.R. Freeman, and S. Waddell, eds. (Cold Spring Harbor: Cold Spring Harbor Laboratory Press).

Pavlov, I.P. (1927). Conditioned Reflexes: An Investigation of the Physiological Activity of the Cerebral Cortex. Lecture IV: Delay (London: Oxford University Press).

Perry, C.J., and Barron, A.B. (2013). Neural mechanisms of reward in insects. Annu. Rev. Entomol. *58*, 543–562.

Prokop, P., and Vaclav, R. (2005). Males respond to the risk of sperm competition in the sexually cannibalistic praying mantis, *Mantis religiosa*. Ethology *111*, 836–848.

Pulver, S.R., Pashkovski, S.L., Hornstein, N.J., Garrity, P.A., and Griffith, L.C. (2009). Temporal dynamics of neuronal activation by Channelrhodopsin-2 and TRPA1 determine behavioral output in *Drosophila* larvae. J. Neurophysiol. *101*, 3075–3088.

Rideout, E.J., Dornan, A.J., Neville, M.C., Eadie, S., and Goodwin, S.F. (2010). Control of sexual differentiation and behavior by the *doublesex* gene in *Drosophila melanogaster*. Nat. Neurosci. *13*, 458–466.

Roeder, K.D. (1935). An experimental analysis of the sexual behavior of the praying mantis (*Mantis religiosa* L.). Biol. Bull. *69*, 203–220.

Rubin, H.B., and Azrin, N.H. (1967). Temporal patterns of sexual behavior in rabbits as determined by an automatic recording technique. J. Exp. Anal. Behav. *10*, 219–231.

Starz-Gaiano, M., Cho, N.K., Forbes, A., and Lehmann, R. (2001). Spatially restricted activity of a *Drosophila* lipid phosphatase guides migrating germ cells. Development *128*, 983–991.

Sweeney, S.T., Broadie, K., Keane, J., Niemann, H., and O'Kane, C.J. (1995). Targeted expression of tetanus toxin light chain in *Drosophila* specifically eliminates synaptic transmission and causes behavioral defects. Neuron *14*, 341–351.

Tayler, T.D., Pacheco, D.A., Hergarden, A.C., Murthy, M., and Anderson, D.J. (2012). A neuropeptide circuit that coordinates sperm transfer and copulation duration in *Drosophila*. Proc. Natl. Acad. Sci. USA *109*, 20697–20702.

Wigby, S., Sirot, L.K., Linklater, J.R., Buehner, N., Calboli, F.C., Bretman, A., Wolfner, M.F., and Chapman, T. (2009). Seminal fluid protein allocation and male reproductive success. Curr. Biol. *19*, 751–757.

Wise, R.A. (2004). Dopamine, learning and motivation. Nat. Rev. Neurosci. *5*, 483–494.

Xue, L., and Noll, M. (2000). *Drosophila* female sexual behavior induced by sterile males showing copulation complementation. Proc. Natl. Acad. Sci. USA *97*, 3272–3275.

Yang, C.H., Rumpf, S., Xiang, Y., Gordon, M.D., Song, W., Jan, L.Y., and Jan, Y.N. (2009). Control of the postmating behavioral switch in *Drosophila* females by internal sensory neurons. Neuron *61*, 519–526.

Yu, J.Y., Kanai, M.I., Demir, E., Jefferis, G.S., and Dickson, B.J. (2010). Cellular organization of the neural circuit that drives *Drosophila* courtship behavior. Curr. Biol. *20*, 1602–1614.

EXTENDED EXPERIMENTAL PROCEDURES

Fly Stocks

Wild-Type Stocks

The wild-type Berlin stock originally from Martin Heisenberg was used as wild-type. For copulation duration assays, virgin females were from the w^{1118} "virginator" strain, which contains a heat shock-inducible *hid* transgene inserted on the Y chromosome that selectively kills males (Starz-Gaiano et al., 2001) (Bloomington *Drosophila* Stock Center #24638).

To generate w^{1118} virgin females, we heat shocked bottles of the w^{1118}/Dp(2;Y)G, P(hs-hid)Y "virginator" strain (Starz-Gaiano et al., 2001) (#24638 Bloomington Stock Center) for 2 hr at 37°C shortly before eclosion. This strain contains a heat shock-inducible *hid* transgene inserted on the Y chromosome that selectively kills males. w^{1118} virgin females were 3-13 days old.

Wild-type Berlin females were used for fertility experiments to avoid potential fertility effects of the heat shock required for generating "virginator" females. Males for fertility experiments were generated as follows: Spermless son-of-*tudor* males (Xue and Noll, 2000) were the male progeny resulting from crossing non-*CyO* females from the tud^1 bw^1 sp^1/*CyO, l(2)DTS513*^{1} (Bloomington #1786) stock to wild-type Berlin males. Males lacking accessory glands were the result of a partial genomic rescue of $paired^{2.45}$ mutants (Bertuccioli et al., 1996; Xue and Noll, 2000) (kindly provided by Markus Noll; University of Zurich). Non-*CyO* males were selected from a +; $paired^{2.45}$/*Cyo; prdRes*/+ stock, where *prdRes* is a genomic fragment of the *paired* locus.

Gal4 Lines

NP5270 (*Drosophila* Genome Resource Center, DGRC #113657); NP3037 (DGRC #113073); NP7323 (DGRC# 105426); NP0967 (DGRC# 112292); NP0525 (DGRC #112198); NP2719 (DGRC #113024). Two other Gal4 insertions available from DGRC (NP0969 and NP7325) gave phenotypes similar to the six Gal4 lines described here (data not shown), but were not discussed because they have insertion sites identical to NP0679 and NP3037, respectively. TH-Gal4 was obtained from the Bloomington stock center (#8848).

Gal80 Lines

ElavGal80 was a gift from Yuh Nung Jan (UCSF). TshGal80 was a gift from Julie Simpson (HHMI-Janelia Farm Research Campus). RepoGal80 was a gift from Tzumin Lee (HHMI-Janelia Farm Research Campus).

UAS Lines

Two different insertions of UAS-Tnt were tested (UAS-TntG and UAS-TntE) (Sweeney et al., 1995) and both gave copulation duration phenotypes when crossed to the Gal4 lines described above (162 ± 11 min for NP5270 > TntG, 96 ± 12 min for NP5270 > TntE). UAS-TntG phenotypes were slightly stronger and was used in all experiments except for the fertility and circadian rhythm assays, where UAS-TntE was used because the UAS-TntG transgene caused reduced fertility and erratic circadian rhythms in the absence of Gal4 (data not shown). Other UAS lines used were: UAS-ImpTnt-V (Inactive Tnt) (Sweeney et al., 1995); UAS-TrpA1 (Bloomington #26263); UAS-nsyb-GFP (Estes et al., 2000); UAS-CD8-GFP (Lee and Luo, 1999); UAS-Dsx-RNAi (Bloomington # 26716), UAS-Gad1-RNAi (VDRC #32344), UAS-VGAT-RNAi (VDRC #103586). When tested as parental controls, UAS stocks were tested as hemizygotes after crossing to w^{1118}.

Dopamine Receptor Mutants

Deletion mutants of DopR1 (DopR1^{attp}) and DopR2 (DopR2^{attp}) and the Canton-S background strain into which they were introgressed were donated by Barry Dickson (Keleman et al., 2012). The PBac insertion into DopEcR (DopEcR^{c02142}) was donated by David Anderson (Inagaki et al., 2012). The PBac insertion into D2R (D2R^{f06521}) was obtained from the Harvard stock center. Both DopEcR^{c02142} and D2R^{f06521} were introgressed by backcrossing for five generations into the Vosshall lab w^{1118} background.

Detailed genotypes of all strains used in the paper are as follows:

Figure 1A

Males

w^{1118}/Y; NP5270/+; UAS-CD8-GFP/+
+/Y; UAS-TntG/+; +/+
+/Y; NP5270/UAS-TntG; +/+
w^{1118}/Y; NP5270; UAS-ImpTnt-V/+

Females

w^{1118}/w^{1118}; +/+; +/+

Figure 1B

Males

+/Y; NP5270/UAS-TntG; +/+

Females

Wild-type Berlin

Figure 1C

Males

w^{1118}/Y; NP5270/UAS-TrpA1; +/+
w^{1118}/Y; UAS-TrpA1/+; +/+
w^{1118}/Y; NP5270/+; UAS-CD8-GFP/+

Females

w^{1118}/w^{1118}; +/+; +/+

Figure 1D

Males

w^{1118}/Y; NP5270/+; UAS-CD8-GFP/+
+/Y; NP5270/RepoGal80; UAS-CD8-GFP/+
+/Y; NP5270/TshGal80; UAS-CD8-GFP/+

Figure 1E

Males

+/Y; NP5270/UAS-TntG; +/+
w^{1118}/Y; NP5270, RepoGal80/UAS-TntG; +/+
w^{1118}/Y; NP5270/UAS-TntG; ElavGal80/+
w^{1118}/Y; NP5270, TshGal80/UAS-TntG; +

Females

w^{1118}/w^{1118}; +/+; +/+

Figure 1F

Males

Wild-type Berlin

Females

w^{1118}/w^{1118}; +/+; +/+

Figure 1G

Males

Wild-type Berlin

Females

w^{1118}/w^{1118}; +/+; +/+ (Experiment)
Wild-type Berlin (Pictured)

Figure 2A

Males

Wild-type Berlin
son-of-*tudor*: Male progeny resulting from crossing non-CyO females from the tud^1 bw^1 sp^1/*CyO, l(2)DTS513*^{1} stock to wild-type Berlin males.
paired rescue: Non-CyO males were selected from a *+; paired*$^{2.45}$*/Cyo; prdRes*/+ stock, where *prdRes* is a genomic fragment of the *paired* locus.

Females

Wild-type Berlin

Figure 2B
Males

w^{1118}/Y; NP5270/+; UAS-CD8-GFP/+

Females

Wild-type Berlin

Figure 2C
Males

w^{1118}/Y; NP5270/+; UAS-CD8-GFP/+

Females

Wild-type Berlin

Figure 2D
Males

w^{1118}/Y; NP5270/+; UAS-CD8-GFP/+
+/Y; UAS-TntE/+; +/+
+/Y; NP5270/UAS-TntE; +/+

Females

Wild-type Berlin

Figure 2E
Males

w^{1118}/Y; NP5270/UAS-TrpA1; +/+
w^{1118}/Y; UAS-TrpA1/+; +/+
w^{1118}/Y; NP5270/+; UAS-CD8-GFP/+

Females

Wild-type Berlin

Figure 2F
Males

w^{1118}/Y; NP5270/UAS-TrpA1; +/+
w^{1118}/Y; UAS-TrpA1/+; +/+
w^{1118}/Y; NP5270/+; UAS-CD8-GFP/+

Females

Wild-type Berlin

Figure 3A
Males

Wild-type Berlin

Figure 3B
Males

Wild-type Berlin

Females

w^{1118}/w^{1118}; +/+; +/+

Figure 3C

Males

w^{1118}/Y; NP5270/+; UAS-CD8-GFP/+
+/Y; UAS-TntG/+; +/+
+/Y; NP5270/UAS-TntG/+; +/+

Females

w^{1118}/w^{1118}; +/+; +/+

Figure 3D

Males

w^{1118}/Y; NP5270/+; UAS-CD8-GFP/+
+/Y; UAS-TntG/+; +/+
+/Y; NP5270/UAS-TntG/+; +/+

Figure 3E

Males

Wild-type Berlin

Females

w^{1118}/w^{1118}; +/+; +/+

Figure 3F

Males

w^{1118}/Y; NP5270/+; UAS-CD8-GFP/+
+/Y; UAS-TntG/+;+/+
+/Y; NP5270/UAS-TntG/+;+/+

Females

w^{1118}/w^{1118}; +/+; +/+

Figure 3G

Males

w^{1118}/Y; NP5270/+; UAS-CD8-GFP/+
w^{1118}/Y; UAS-TrpA1/+;+/+
w^{1118}/Y; NP5270/UAS-TrpA1/+;+/+

Females

w^{1118}/w^{1118}; +/+; +/+

Figure 4B

Males

+/Y; UAS-TntG/+; +/+
+/Y; NP5270/UAS-TntG; +/+
+/Y; NP7323/UAS-TntG; +/+
+/Y; NP0525/UAS-TntG; +/+
+/Y; NP3037/UAS-TntG; +/+
+/Y; NP0697/UAS-TntG; +/+
+/Y; NP2719/UAS-TntG; +/+

Females

w^{1118}/w^{1118}; +/+; +/+

Figure 4C
Males

w^{1118}/Y; NP5270/RepoGal80; UAS-CD8-GFP/+
w^{1118}/Y; NP7323/RepoGal80; UAS-CD8-GFP/+
w^{1118}/Y; NP0525/RepoGal80; UAS-CD8-GFP/+
w^{1118}/Y; NP3037/RepoGal80; UAS-CD8-GFP/+
w^{1118}/Y; NP0697/RepoGal80; UAS-CD8-GFP/+
w^{1118}/Y; NP2719/RepoGal80; UAS-CD8-GFP/+

Figure 5A
Males

w^{1118}/Y; NP2719/RepoGal80; UAS-CD8-GFP/+

Figure 5B
Males

w^{1118}/Y; NP2719/RepoGal80; UAS-CD8-GFP/+

Figure 5C
Males

w^{1118}/Y; NP2719/RepoGal80; UAS-nsyb-GFP/+

Figure 5D
Males

w^{1118}/Y; NP2719/UAS-TrpA1; +/+
w^{1118}/Y; UAS-TrpA1/+; +/+
w^{1118}/Y; NP2719/+; UAS-CD8-GFP/+

Females

w^{1118}/w^{1118}; +/+; +/+

Figure 5E
Males

UAS-Dicer2/Y; NP2719/+; UAS-CD8-GFP/+
w^{1118}/Y; +/+; UAS-Gad1-RNAi/+
UAS-Dicer2/Y; NP2719/+; UAS-Gad1-RNAi/+
w^{1118}/Y; UAS-VGAT-RNAi/+; +/+
UAS-Dicer2/Y; NP2719/UAS-VGAT-RNAi; +/+

Females

w^{1118}/w^{1118}; +/+; +/+

Figure 5F
Males

w^{1118}/Y; NP2719/RepoGal80; UAS-CD8-GFP/+

Figure 5G
Males

w^{1118}/Y; NP2719/RepoGal80; UAS-CD8-GFP/+
w^{1118}/Y; NP2719/RepoGal80; UAS-CD8-GFP/UAS-Gad1-RNAi

Figure 5H
Males

UAS-Dicer2/Y; NP2719/+; UAS-Gad1-RNAi/+

UAS-Dicer2/Y; NP2719/UAS-TrpA1; +/+
UAS-Dicer2/Y; NP2719/UAS-TrpA1; UAS-Gad1-RNAi/+

Figure 6A
Male

w^{1118}/Y; NP5270/RepoGal80; UAS-CD8-GFP/+

Female

w^{1118}/ w^{1118}; NP5270/RepoGal80; UAS-CD8-GFP/+

Figure 6B
Male

w^{1118}/Y; NP2719/RepoGal80; UAS-CD8-GFP/+

Female

w^{1118}/ w^{1118}; NP2719/RepoGal80; UAS-CD8-GFP/+

Figure 6C
Males

w^{1118}/Y; NP2719/RepoGal80; UAS-CD8-GFP/+

Figure 6D
Males

w^{1118}/Y; NP2719/RepoGal80; UAS-CD8-GFP/+

Figure 6E
Males

$Elav^{C155}$/Y; UAS>stop>CD8-GFP/+; Fru-Flp/+
w^{1118}/Y; UAS>stop>CD8-GFP/NP5270; Fru-Flp/+
w^{1118}/Y; UAS>stop>CD8-GFP/NP2719; Fru-Flp/+

Figure 6F
Males

UAS-Dicer2/Y; NP5270/RepoGal80; UAS-CD8-GFP/UAS-DsxRNAi
UAS-Dicer2/Y; NP2719/RepoGal80; UAS-CD8-GFP/UAS-DsxRNAi

Figure 7A
Males

w^{1118}/Y; UAS-TrpA1/+; TH-Gal4/+
w^{1118}/Y; +/+; TH-Gal4/UAS-CD8-GFP
w^{1118}/Y; UAS-TrpA1/+; +/+

Females

w^{1118}/w^{1118}; +/+; +/+

Figure 7B
Males

w^{1118}/Y; UAS-TrpA1/+; TH-Gal4/+
w^{1118}/Y; +/+; TH-Gal4/UAS-CD8-GFP
w^{1118}/Y; UAS-TrpA1/+; +/+

Females

w^{1118}/w^{1118}; +/+; +/+

Figure 7C

Males

w^{1118}/Y; +/+; TH-Gal4/UAS-CD8-GFP
w^{1118}/Y; TshGal80/+; TH-Gal4/UAS-CD8-GFP

Figure 7D

Males

w^{1118}/Y; UAS-TrpA1/+; TH-Gal4/+
w^{1118}/Y; UAS-TrpA1/TshGal80; TH-Gal4/+

Females

w^{1118}/w^{1118}; +/+; +/+

Figure 7E

Males

Canton-S
+/+; +/+; $DopR1^{attp}$

Females

w^{1118}/w^{1118}; +/+; +/+

Figure 7F

Males

w^{1118}/Y; +/+; +/+
$DopEcR^{c02142}$

Females

w^{1118}/w^{1118}; +/+; +/+

Figure 7G

Males

$D2R^{f06521}$
w^{1118}/Y; +/+; +/+

Females

w^{1118}/w^{1118}; +/+; +/+

Figure 7H

Males

Canton-S
+/+; +/+; $DopR2^{attp}$

Females

w^{1118}/w^{1118}; +/+; +/+

Figure 7I

Males

w^{1118}/Y; UAS-TrpA1/+; TH-Gal4/+
w^{1118}/Y; NP2719/UAS-TrpA1; +/+
w^{1118}/Y; NP2719/UAS-TrpA1; TH-Gal4/+

w^{1118}/Y; NP2719/+; TH-Gal4/UAS-CD8-GFP
w^{1118}/Y; UAS-TrpA1/+; +/+

Females

w^{1118}/w^{1118}; +/+; +/+

Figure 7J
Male

w^{1118}/Y; NP2719/RepoGal80; UAS-CD8-GFP/+

Immunostaining and Microscopy

For most staining, animals were fixed by incubation in 4% paraformaldehyde in phosphate-buffered saline (PBS) plus 0.1% Triton for 1 hr at room temperature. For VNC preparations, flies were decapitated prior to fixation to allow penetration of fixative. Brains and VNCs were dissected free of cuticle, fat body, trachea and were incubated with primary antibodies diluted in 5% goat serum, 0.1% Triton X-100 in PBS for 40 hr at 4°C. Samples were washed 3 times over 6 hr in PBT (PBS and 0.1% Triton X-100) at room temperature before application of secondary antibodies for 40 hr at 4°C. Samples were washed 3 times over 3-8 hr in PBT (PBS and 0.1% Triton X-100) and the samples were mounted with VectaShield (Vector Labs) between two glass coverslips with bridging glass coverslips so that both sides of the tissue could be imaged. Confocal sections were acquired using a Zeiss LSM510 confocal microscope at 3μm intervals and maximum projections of image stacks were performed in ImageJ (NIH; http://rsbweb.nih.gov/ij/). For colabeling experiments with anti-FruM, anti-DsxM and anti-GABA, 1 μm optical sections were analyzed and quantified. For anti-GABA staining, brains and VNCs were dissected first, then fixed by incubation for 20 min at room temperature in 4% paraformaldehyde without Trition-X-100, after which the samples were stained and prepared as described above.

Antibodies

Rabbit anti-GFP (CAT# A-11122, Invitrogen, 1:1000 dilution); Mouse anti-GFP (CAT# A-11120, Invitrogen, 1:100 dilution); Mouse anti-nc82 (Developmental Studies Hybridoma Bank; 1:7 dilution, developed under the auspices of the NICHD and maintained by The University of Iowa, Department of Biology, Iowa City, IA 52242); Rabbit anti-FruM "male2" (Kimura et al., 2008) (1:500 dilution); Rat anti-DsxM (Hempel and Oliver, 2007) (1:500 dilution); Rabbit anti-GABA (1:1000; Sigma-Aldrich CAT#A2052); Mouse anti-rat tyrosine hydroxylase (TH) (1:500 ImmunoStar CAT#22941). Secondary fluorescent antibodies were AlexaFluor Goat anti-Rabbit (1:500 dilution; Invitrogen CAT#11008), AlexaFluor Goat anti-Mouse (1:500 dilution; Invitrogen CAT#A-11001), Cy3 Goat Anti-Mouse (1:205 dilution; Jackson ImmunoResearch CAT#115-165-166), Cy3 Goat Anti-Rat (1:205 dilution; Jackson ImmunoResearch CAT#112-165-143), Cy3 Goat Anti-Rabbit (1:205 dilution; Jackson ImmunoResearch CAT#111-165-144).